Paraffin/Bamboo Carbon Composites for Electrical Vehicle Battery Thermal Management

I Made Arsawan[1,2,3], I Dewa Gede Ary Subagia[2,3,*], I Ketut Gede Wirawan[2], Dewa Ngakan Ketut Putra Negara[2]

[1]Mechanical Engineering Department, Politeknik Negeri Bali, Bali, Indonesia

[2]Study Program of Mechanical Engineering, Engineering Faculty, Udayana University, Bali, Indonesia

[3]Engineering Materials Laboratory, Engineering Faculty, Udayana University, Bali, Indonesia

Received 01 October 2025; received in revised form 01 January 2026; accepted 05 January 2026

DOI: https://doi.org/10.46604/ijeti.2026.15749

Abstract

This study aims to develop a paraffin-based phase change material (PCM) modified with bamboo waste carbon (BWC). The modification is intended to enhance the performance of a passive battery thermal management system for electric vehicles. PCM composites containing 0, 5, 10, and 15 wt.% BWC are prepared and characterized using simultaneous thermal analysis, fourier transform infrared spectroscopy, and scanning electron microscopy. The thermal performance of the composites is evaluated through battery module cooling simulations under a constant discharge load. The simulations assess the ability of the PCM composites to maintain battery operating temperatures within a safe range (293.15–313.15 K). The results indicate that the composite containing 10 wt.% BWC achieves optimal performance, with a 33.9% increase in thermal energy absorption. The peak battery temperature is reduced to 309.03 K. These findings demonstrate BWC's potential as an effective and sustainable thermal additive for paraffin-based PCMs in passive BTMS applications for electric vehicles.

Keywords: phase change material (PCM), bamboo waste carbon (BWC), battery thermal management, electric vehicles

1. Introduction

Battery performance and service life are critical factors in the thermal management of electric vehicles. During operation, lithium-ion batteries generate substantial heat due to electrochemical reactions and internal resistance. This excessive heat can increase operating temperatures and reduce energy efficiency. It also accelerates cell degradation, and in extreme cases, leads to thermal runaway. Consequently, developing effective and sustainable battery thermal management systems (BTMSs) has become a central research focus in modern electric vehicle technology [1-2].

A promising approach to mitigate heat accumulation in battery systems is the use of phase change materials (PCMs). Such materials can absorb and release substantial thermal energy through latent heat during phase transitions. This capability helps to stabilize battery operating temperatures [3-4]. Compared with conventional cooling strategies, PCMs offer several advantages. These include a high thermal energy storage capacity, passive operation without additional energy consumption, and the ability to maintain nearly a constant temperature during the melting process [5]. Among various PCMs, paraffin wax has been widely employed due to its high latent heat, good chemical stability, and relatively low cost [6-7]. However, its major

* Corresponding author. E-mail address: arsubmt@unud.ac.id

limitation is intrinsically low thermal conductivity (approximately 0.2–0.4 W/m·K), which results in slow heat diffusion and non-uniform temperature distribution within battery modules [8].

To overcome this limitation, numerous studies have focused on enhancing paraffin-based PCMs. One common approach involves incorporating thermally conductive carbon-based materials, such as graphite, carbon nanotubes, graphene, and metallic fibers. Mane et al. [9] reported improved temperature uniformity in battery modules when using expandable graphite, while Zhang et al. [10] demonstrated up to a 30-fold increase in thermal conductivity through the integration of graphite fins. Other studies have also shown improved thermal stability and heat distribution using engineered carbon structures [11-12]. Despite these advances, most conventional carbon additives are expensive, have complex fabrication processes, and can have significant environmental impacts. These challenges highlight the growing demand for cost-effective and environmentally friendly thermal enhancers that can deliver competitive performance.

In response to concerns related to cost, complex synthesis protocols, and sustainability, recent research has increasingly explored alternative carbon sources derived from biomass. Bamboo-derived carbon, particularly bamboo waste carbon (BWC), has emerged as a promising candidate due to bamboo's rapid growth and high carbon content. Through carbonization, bamboo is converted into porous bio-carbon with a large specific surface area, improved thermal conductivity, and a strong heat adsorption capability [13]. Although several studies have demonstrated the potential of bamboo-based bio-carbon in thermal energy storage applications, its specific application as a thermal additive in paraffin-based PCM composites for lithium-ion battery cooling in electric vehicles remains limited. Furthermore, few studies have examined how variations in bamboo carbon content influence thermal properties, chemical structure, microstructural morphology, as well as how these material characteristics affect system-level battery cooling performance.

To address these research gaps, this study develops paraffin-based PCM composites modified with BWC at a mass fraction of 0%, 5%, 10%, or 15%. This work is novel for several reasons:

(1) It develops a sustainable, low-cost, and porous BWC-reinforced paraffin PCM for passive BTMS applications in electric vehicles.
(2) It provides comprehensive characterization using simultaneous thermal analysis (STA) for thermal properties, fourier transform infrared spectroscopy (FTIR) for chemical structure and compatibility, and scanning electron microscopy (SEM) for microstructure and elemental distribution, revealing material interactions and performance-enhancement mechanisms.
(3) It evaluates cooling performance through constant-current discharge simulations of a battery module. This provides experimental evidence that bio-composite PCMs stabilize battery temperatures. In addition, the study establishes a correlation between material properties and system-level cooling performance, offering scientific guidance for the design of biomass-based passive BTMSs. The findings are expected to confirm the potential of BWC as a viable and sustainable thermal additive for next-generation battery thermal management systems.

2. Methodology

This section describes the materials used in this study, along with the preparation of bamboo carbon and the fabrication of PCM composites. The characterization techniques used to examine the thermal and structural properties are then presented. Finally, the experimental design and analytical methods employed to evaluate the thermal performance of the developed PCM composites are introduced.

2.1 Material

The primary materials used in this study are paraffin wax as the base PCM and BWC as a thermal conductivity enhancer. Paraffin wax is supplied by PT Aneka Kimia Inti (Indonesia), and its physicochemical properties are summarized in Table 1.

Table 1 Characterization of the paraffin wax [14]

Melting Temperature (K)	Heat of Fusion (kJ/kg)	Thermal Conductivity (W/m·K)	Density (kg/m³)
337 (64 ℃)	266	0.339 (solid, 318 K [45.7 ℃])	916 (solid, 297 K [24 ℃])

Bamboo carbon is produced from bamboo waste collected from small-scale handicraft industries in Bali Province, Indonesia. The raw bamboo waste is subjected to pyrolysis at 673 K to obtain a porous, carbon-rich material. The resulting bamboo carbon exhibits a well-developed porous structure and enhanced thermal conductivity. These properties make it suitable as a filler for improving heat-transfer performance in paraffin-based PCM composites.

The utilization of BWC provides a low-cost and sustainable alternative to conventional carbon additives. This approach promotes the valorization of biomass waste by converting industrial by-products into functional materials. Such a strategy reduces environmental impact and improves the thermal management efficiency of lithium-ion batteries.

2.2 Preparation of bamboo carbon

Fig. 1 presents the preparation procedure of bamboo-derived carbon. Initially, bamboo waste is cut into rectangular pieces with approximate dimensions of 0.05 m × 0.01 m × 0.002 m. The samples are thoroughly washed with distilled water to remove surface contaminants and impurities. They are then air-dried under direct sunlight for 5 h. Subsequently, the bamboo pieces are oven-dried at 373 K for 2 h to eliminate residual moisture. The dried bamboo is carbonized in a muffle furnace at 673 K for 2 h in an oxygen-limited environment. To ensure complete carbonization and prevent oxidation, the samples are allowed to cool naturally inside the furnace until the internal temperature reaches room temperature (298 K). The resulting bamboo carbon is mechanically ground into a fine powder and sieved through a 50-μm mesh. This process obtains a uniform particle size distribution. Finally, the carbon powder is stored in an airtight container to prevent moisture absorption and contamination prior to incorporation into the PCM composite.

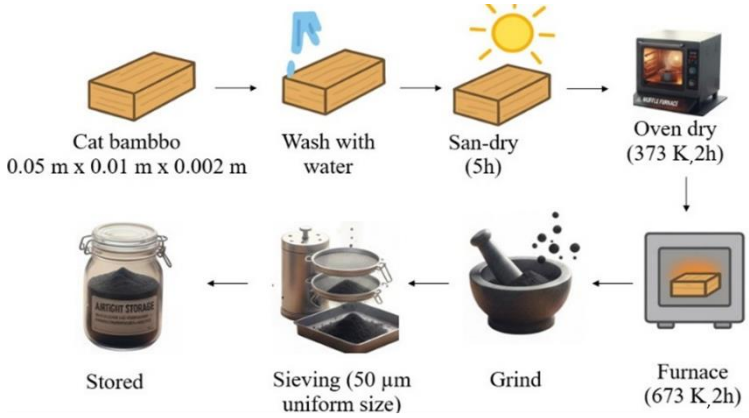

Fig. 1 Bamboo-derived carbon preparation process

2.3 Preparation of PCM composites

The preparation of the PCM composite begins with the primary materials: paraffin as the PCM matrix and BWC as a filler to enhance thermal conductivity (Fig. 2(a)). In the initial stage, the paraffin is melted at 343 K for 60 min until completely molten (Fig. 2(b)). Then, the molten paraffin is mechanically stirred at 250 rpm, while the temperature is maintained at 343 K to prevent agglomeration. Subsequently, BWC is gradually added to the molten paraffin according to the mixture compositions listed in Table 2 (Fig. 2(c)). The mixing process is carried out at 250 rpm for 120 min until a homogeneous PCM composite is obtained, with no visible agglomerates (Fig. 2(d)).

The next stage involves molding the PCM composite into predefined molds. Two types of molds are used. The first mold is designed for material characterization tests, with a sample mass of 0.1 g for each PCM composite. The second mold is used

for PCM performance testing, with a sample mass of 300 g for each composite (Fig. 2(e)). After molding, the samples are cooled and stabilized in a desiccator at 300 K for 24 h before further testing.

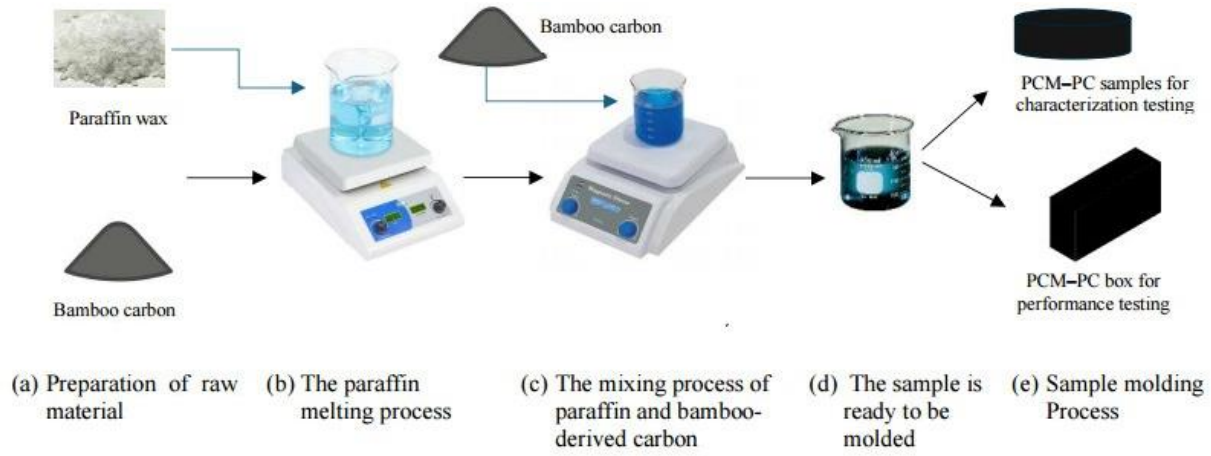

Fig. 2 Preparation of the PCM composites

Table 2 Sample composition

Sample Number	Sample Code	Sample Name	Paraffin Wax (wt.%)	BWC (wt.%)
1	PCM PP	Pure Paraffin	100	0
2	PCM PC 5%	Paraffin with 5 wt.% BWC	95	5
3	PCM PC 10%	Paraffin with 10 wt.% BWC	90	10
4	PCM PC 15%	Paraffin with 15 wt.% BWC	85	15

2.4 Material characterization

The characteristics of the PCM composites are analyzed using STA, specifically a NEXTA STA instrument (STA200RV, Hitachi, Japan). Changes in the material mass as a function of temperature are evaluated through thermogravimetric analysis (TGA), while thermal energy–related characteristics are examined using differential scanning calorimetry (DSC). The surface morphology of pure PCM and the PCM composites is examined using a scanning electron microscope (SEM) (JEOL JSM 6510LA). The morphology of pure BWC is also analyzed for comparison. FTIR is used to identify functional groups in pure PCM, pure BWC, and PCM-BWC composites (FTIR-8400S, Shimadzu, Japan).

2.5 Experimental design

Fig. 3 illustrates the dummy testing system used to evaluate the performance of PCM composites as a passive cooling system for electric vehicle batteries. The dummy battery is placed inside a PCM composite box (Fig. 3(a)), which is filled with 300 g of PCM composite prepared according to Table 2. The PCM box is fabricated from aluminum and has dimensions of 0.140 m × 0.080 m × 0.040 m and a wall thickness of 0.0005 m (Fig. 3(b)).

The temperature distribution within the cooling system is measured using Type-K thermocouples (020101, Viara Ido Teknik, Indonesia). The positions of the thermocouples are illustrated in Fig. 3(c). The thermocouples are connected to a data logger that records temperature data at 60-s intervals. The dummy battery serves as the heat source and is powered by a DC supply with an AC input voltage of 115 V ± 10% or 230 V ± 10%. The testing system operates between 273.15–313.15 K with a relative humidity below 80%. Finally, the storage temperature range is 273.15–343.15 K with a relative humidity below 70%.

A heating element with a power rating of 5 W is employed to simulate heat generation during battery operation. The heating element reaches a temperature of 323.53 K within 3600 s. This value falls within the typical thermal operating range of lithium-ion batteries (288.15–323.15 K).

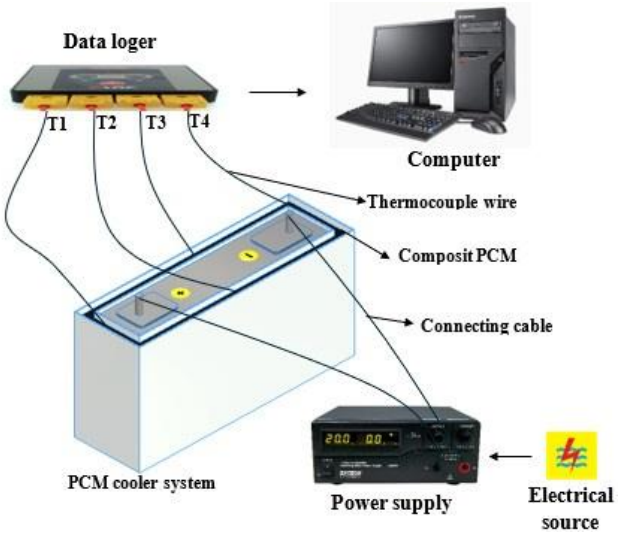

(a) Experimental setup

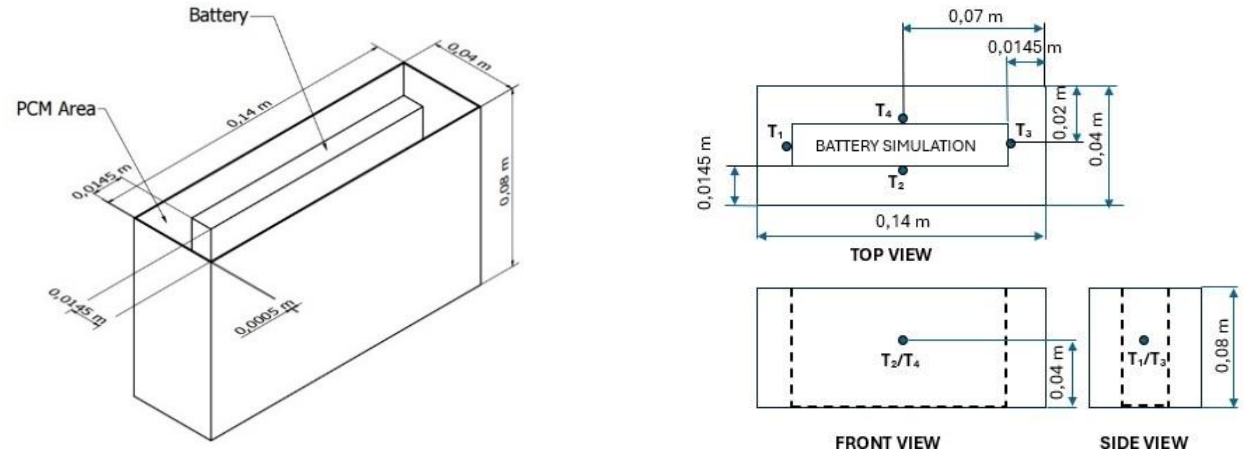

(b) Geometric dimensions (c) Thermocouple locations,

Fig. 3 Proposed BTMS

2.6 Analytical methods

FTIR is employed to identify functional groups and to evaluate potential chemical interactions between paraffin and BWC within the PCM composites. The analysis involves identifying characteristic absorption peaks within the wavenumber range of 4000–500 cm^{-1} for pure paraffin, BWC, and each composite sample. The composite spectra are compared with pure paraffin to examine new absorption bands, peak position shifts, and peak intensity variations. These features may indicate intermolecular interactions or structural modifications induced by the incorporation of bamboo carbon.

SEM is conducted to investigate the surface morphology and dispersion behavior of BWC particles within the paraffin matrix. The evaluation focuses on observing the overall surface morphology, porosity, particle size, and particle shape, as well as identifying potential particle agglomeration. In addition, the spatial distribution of BWC within the matrix is examined to determine whether the particles are homogeneously dispersed or locally concentrated. The observed microstructural features are interpreted to assess three key aspects: (i) the physical bonding between paraffin and BWC, (ii) the degree of particle embedding, and (iii) the resulting impact on heat transfer enhancement.

Thermal characterization of the PCM composites is performed using STA, which integrates TGA and DSC. TGA is employed to evaluate the thermal stability and mass loss behavior of the samples as a function of temperature. Meanwhile, DSC is used to determine phase transition temperatures, latent heat (enthalpy of fusion, [ΔH]), and the specific heat capacity (Cp) of the PCM composites. These thermal parameters are calculated as follows:

$$Q = m \cdot Cp \cdot \Delta T \tag{1}$$

$$Cp = \frac{Q}{m \cdot \Delta T} \tag{2}$$

$$Q = m \cdot \Delta H \tag{3}$$

$$Cp = \frac{\Delta H}{\Delta T} \tag{4}$$

where Q represents the amount of heat absorbed or released by the PCM (kJ), ΔH denotes the enthalpy change (kJ/kg), m is the sample mass (kg), Cp is the specific heat capacity (kJ/kg·K), and ΔT is the temperature difference between the onset and endset temperatures (K) for each PCM composite.

3. Results and Discussion

This section presents and discusses the experimental results obtained in this study. The discussion is organized to systematically address the chemical characterization, morphological characterization, thermal characterization, and thermal stability of the PCM composites. Following this, an integrated discussion to interpret the relationships between material characteristics and thermal performance.

3.1 Chemical characterization of the PCM composites

Fig. 4 presents the FTIR spectra of pure paraffin (PCM PP), BWC, and the composites with varying mass fractions of BWC (PCM PC 5%, PCM PC 10%, and PCM PC 15%). Overall, the spectral profiles of the composites closely resemble that of pure PCM. This indicates that the incorporation of BWC does not induce chemical structural changes in paraffin.

For PCM PP, strong absorption bands appear at 2942 and 1472 cm^{-1}, which correspond to C–H stretching and C–H bending vibrations of aliphatic CH_2 groups in the hydrocarbon chains. In addition, the band at 731 cm^{-1} is clearly observed and assigned to CH_2 rocking, a characteristic feature of long-chain alkanes such as paraffin.

The FTIR spectrum of BWC exhibits a broad band around 3618 cm^{-1}, which is attributed to O–H stretching vibrations associated with surface hydroxyl groups and adsorbed moisture within the porous carbon structure. A weak band at approximately 2347 cm^{-1} is assigned to adsorbed CO_2 or combination vibrations. These are commonly observed in carbonaceous materials. These features indicate the presence of surface-active functional groups in BWC, while no dominant absorption bands appear in the fingerprint region.

The spectra of PCM PC 5%, PCM PC 10%, and PCM PC 15% show that the characteristic C–H absorption bands of paraffin remain dominant at 2942 and 1472 cm^{-1}. This confirms that the aliphatic molecular structure of the paraffin matrix is preserved. The reappearance of the O–H band at 3618 cm^{-1} with a reduced intensity further confirms the presence of BWC within the composites without altering the chemical structure of paraffin.

The absence of new absorption bands or the disappearance of major peaks indicates that composite formation is governed by physical interactions rather than chemical reactions. These interactions likely involve surface adsorption, van der Waals forces, and weak hydrogen bonding between the O–H groups of BWC and the hydrocarbon chains of paraffin. This behavior aligns with previous studies on paraffin–carbon composites [15]. In such cases, carbon fillers (e.g., graphene or nanotubes) serve as thermal stabilizers without altering the paraffin's chemical structure. Consequently, the FTIR results confirm that paraffin is physically confined within the porous structure of BWC, forming a chemically stable PCM composite suitable for thermal energy storage applications.

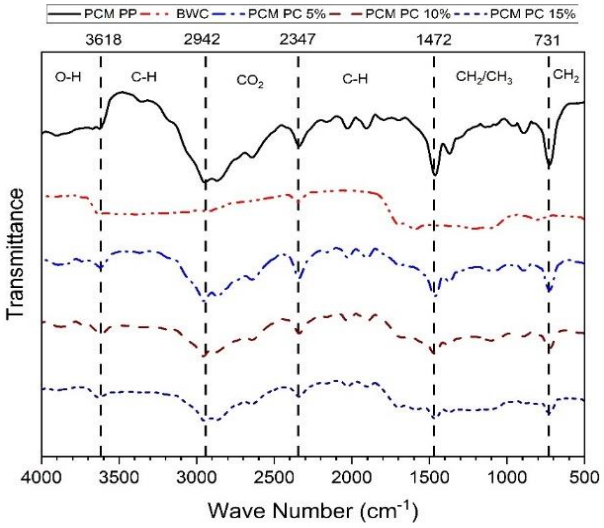

Fig. 4 FTIR spectra of PCM and its composites

3.2 Morphological characterization of the PCM composites

Fig. 5 presents SEM micrographs of BWC, pure paraffin, and a paraffin–BWC composite. In Fig. 5(a), BWC exhibits a porous surface with thin walls and large open cavities. This structure is well-suited for paraffin impregnation because it provides ample space for absorption. In agreement with Huo et al. [12], these characteristic features of biomass-derived carbon provide a high surface area. Consequently, this promotes more effective heat absorption within the composite system.

Pure paraffin, shown in Fig. 5(b), displays a smooth and layered surface, reflecting its typical lamellar crystalline structure and the absence of pores. This morphology indicates high crystallinity, which contributes to thermal stability but inherently limits phonon transport and, consequently, suppresses thermal conductivity. The composite shown in Fig. 5(c) has a denser surface, with carbon pores that are largely covered or filled by paraffin. The smoother regions indicate the presence of paraffin layers adhering to the pore walls. There is no phase separation between carbon and paraffin, suggesting that paraffin is well distributed throughout the carbon matrix. These observations confirm that the physical impregnation process is effective, resulting in a composite structure in which paraffin is retained within the pores of BWC.

Altogether, the FTIR and SEM analyses confirm that BWC is well dispersed and integrated within the paraffin matrix. The FTIR spectra show no new absorption bands or significant peak shifts. This indicates that the interaction between paraffin and bamboo carbon is physical rather than chemical. In addition, the surface morphology shows uniformly distributed carbon particles embedded within the paraffin matrix, further confirming that BWC is effectively incorporated into the PCM composite.

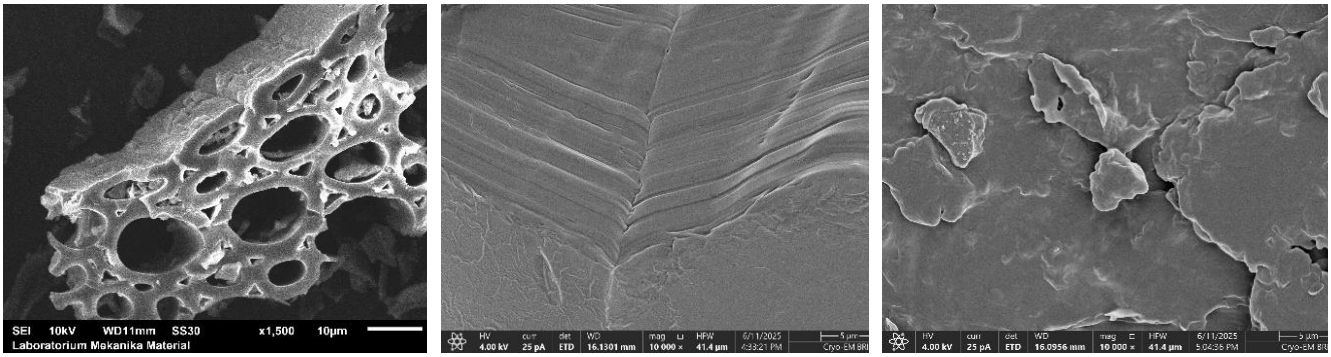

(a) BWC (b) Pure paraffin wax (c) Paraffin-BWC composite

Fig. 5 SEM micrographs of PCM materials

3.3 Thermal characterization of the PCM composites

The DSC curves in Fig. 6 show the thermal properties of PCM PP, PCM PC 5%, PCM PC 10%, and PCM PC 15%. In general, the addition of BWC results in slight variations in the phase transition temperatures. Among the samples, PCM PC 10% exhibits the most pronounced shift toward higher transition temperatures. It has a melting temperature of 336.45 K, an onset temperature of 327.71 K, and an endset temperature of 368.42 K. In contrast, PCM PC 5% shows the lowest onset temperature of 323.18 K.

PCM PC 10% also achieves the highest ΔH (104.99 kJ/kg), whereas ΔH is smaller for PCM PC 5% and PCM PC 15% compared with PCM PP. This reduction is attributed to the decreased fraction of active paraffin caused by the presence of carbon, which does not directly contribute to latent heat storage. The ΔH increase for PCM PC 10% compared with PCM PP indicates optimal impregnation. This enhancement suggests that in this composition, paraffin is uniformly absorbed within the carbon pores. There is no significant loss of latent heat storage capacity. However, ΔH decreases to 89.91 kJ/kg for PCM PC 15% due to excessive confinement of paraffin within the carbon pores, which reduces the effective fraction of active PCM.

These findings are consistent with previous studies on carbon-based PCM composites, which have reported the existence of an optimal additive concentration that maximizes energy storage and enhances thermal conductivity [16]. The results demonstrate that BWC serves as a sustainable and effective additive. It improves the performance of paraffin-based PCMs in thermal management applications for electric vehicle batteries.

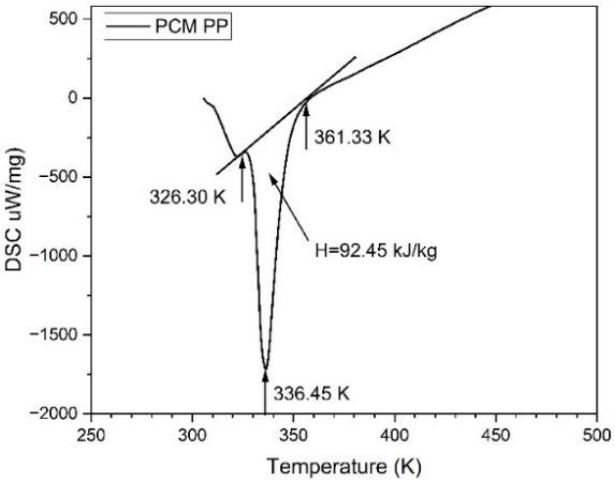

(a) PCM PP

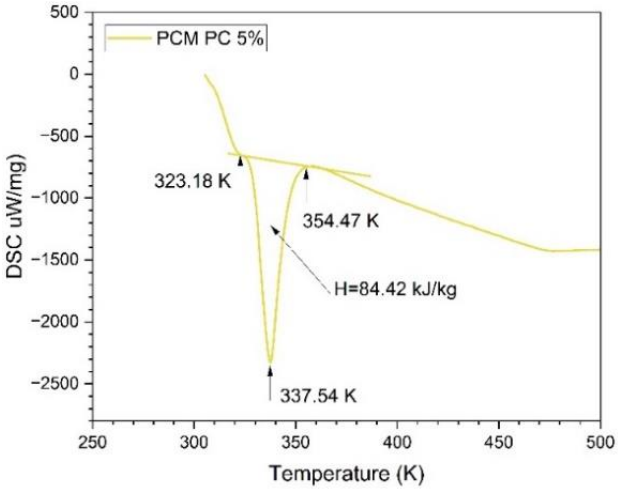

(b) PCM PC 5%

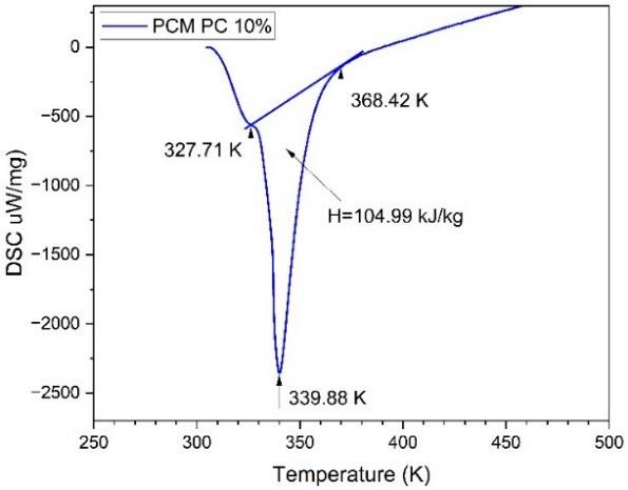

(c) PCM PC 10%

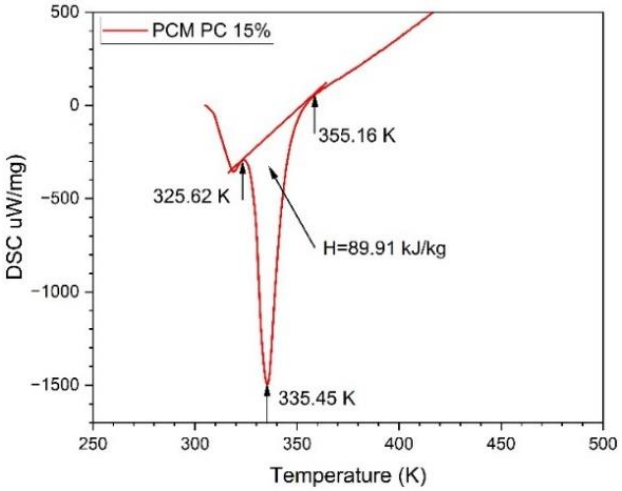

(d) PCM PC 15%

Fig. 6 DSC spectra of PCM and its composites

Table 3 provides the onset melting temperature, melting point, endset melting temperature, ΔH, and ΔT for PCM PP, PCM PC 5%, PCM PC 10%, and PCM PC 15%. Variations in the melting onset temperature of the PCM composites reveal a competitive interplay between enhanced thermal conductivity and the stability of the paraffin crystalline structure. These changes indicate that the melting onset behavior is governed not only by the latent heat storage capacity but also by kinetic and structural factors.

Table 3 Thermal transition parameters of PCM composites

Sample	Onset (K)	Melting Point (K)	Endset (K)	ΔH (kJ/kg)	ΔT (K)
PCM PP 0%	326.30	336.45	361.33	92.45	35.03
PCM PC 5%	323.18	337.54	354.47	84.42	31.29
PCM PC 10%	327.71	339.88	368.42	104.99	40.71
PCM PC 15%	325.62	335.45	355.16	89.91	29.54

PCM PC 5% presents a decrease in the melting onset temperature. This behavior is primarily attributed to enhanced thermal conductivity, which accelerates heat distribution within the PCM matrix and enables the melting of paraffin crystals at lower temperatures. In addition, interfacial interactions between BWC and paraffin disrupt the regularity of paraffin molecular chains, leading to a reduction in crystallinity. Paraffin absorbed within the porous structure of BWC also experiences a micro-confinement effect, which intrinsically lowers its melting temperature compared with bulk paraffin. The combined influence of these factors reduces the melting onset temperature despite the simultaneous increase in thermal conductivity and the Cp of the composite. Therefore, the decrease in the melting onset temperature does not indicate degraded thermal performance. Instead, it reflects improved heat transfer efficiency, which provides a significant advantage for electric vehicle BTMS applications.

For PCM PC 10%, the melting onset temperature increases. This behavior is associated with the attainment of the percolation threshold, where carbon particles form a continuous and highly efficient heat conduction network without significant agglomeration. Under this condition, thermal conductivity is optimally enhanced while the stability of the paraffin crystalline phase is largely preserved. Previous studies [17] confirm that thermal conductivity peaks near this threshold. Conversely, filler contents exceeding this point tend to disrupt heat conduction pathways and compromise the PCM's phase stability.

Similar phenomena have also been observed in biochar-based PCMs, where homogeneous dispersion at an optimal filler fraction provides the best balance between thermal conductivity and latent heat storage capacity [18]. In the context of electric vehicle BTMS, filler fractions near the percolation threshold have been demonstrated to deliver the most effective cooling performance [19]. In contrast, the melting onset temperature decreases for PCM PC 15%. This reduction suggests that carbon loading beyond the percolation threshold disrupts the continuity of the heat conduction network. Furthermore, excessive loading intensifies the confinement effect on the paraffin filler. Such conditions reduce the fraction of thermally active paraffin and diminish the overall thermal stability of the composite.

On the whole, these findings confirm that both the BWC content and the homogeneity of its distribution are critical parameters that govern the thermal behavior and stability of PCM composites. Although carbon incorporation generally improves thermal conductivity and increases heat absorption and release, an increased heat transfer rate does not necessarily lead to a higher ΔH. In PCM PC 5% and PCM PC 15%, the carbon fraction is below and above the optimal range, respectively, resulting in a reduction in enthalpy despite enhanced thermal conductivity. In contrast, PCM PC 10% exhibits the most balanced performance. At this concentration, the carbon content is sufficient to improve thermal conductivity without significantly disrupting the paraffin crystalline structure. Furthermore, the carbon distribution remains highly homogeneous.

Based on the DSC results, ΔH, together with the differences between the onset and endset temperatures, is used to calculate the Cp of each PCM sample using Eq. (4). The calculated Cp values are presented in Fig. 7. The incorporation of

BWC significantly modifies the Cp of the PCM composites. PCM PC 10% demonstrates the highest Cp (2.723 kJ·kg^{-1}·K^{-1}). Note that the Cp is reduced for PCM PC 15%, which can be attributed to the reduced paraffin mass fraction, as paraffin is the primary contributor to latent heat storage. These trends are consistent with the findings reported by Li et al. [20] and Zhou et al. [21].

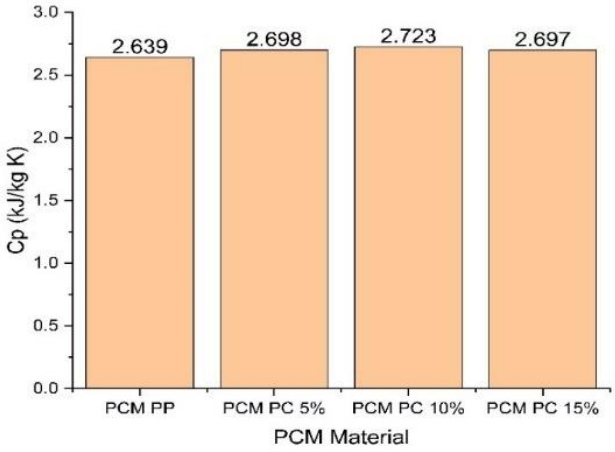

Fig. 7 Specific heat of PCM and its composites

3.4 Thermal stability of the PCM composites

Fig. 8 shows the TGA curves for PCM PP, PCM PC 5%, PCM PC 10%, and PCM PC 15%. All samples exhibit negligible mass loss below 400 K, indicating good thermal stability within the typical operating temperature range of electric vehicle batteries (323–348 K). The incorporation of BWC significantly influences the thermal stability of the PCM composite. Pure paraffin begins to thermally degrade at 463 K. The onset of degradation is delayed to 472 K for PCM PC 5% and 479 K for PCM PC 10%. In contrast, PCM PC 15% shows an earlier degradation onset at 409 K.

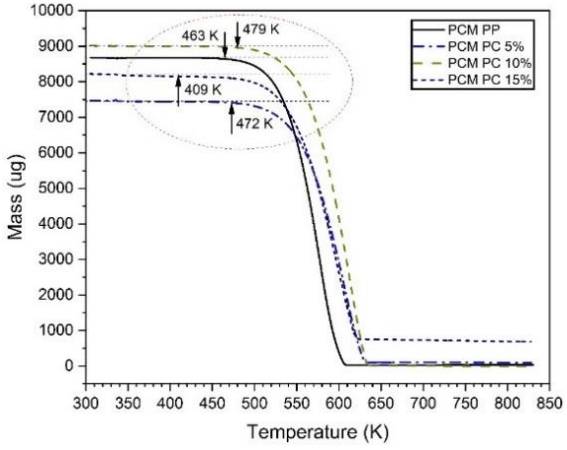

Fig. 8 TGA spectra of PCM and its composites

The reduced degradation temperature observed for PCM PC 15% indicates that higher carbon-based enhancer content does not necessarily enhance thermal stability. At 5 and 10 wt.% BWC, the porous structure of BWC effectively confines paraffin through physical adsorption and pore entrapment. This mechanism suppresses volatilization and successfully delays thermal degradation.

Pore oversaturation occurs at the highest mass fraction (15 wt.%), resulting in weaker confinement of paraffin molecules within the carbon matrix and greater susceptibility to early volatilization. In addition, augmented BWC content introduces more oxygen-containing functional groups and residual reactive sites formed during pyrolysis. At elevated concentrations,

these sites may act as catalytic centers that accelerate thermal oxidation and promote hydrocarbon chain scission. Moreover, the higher thermal conductivity of BWC at high loadings may facilitate localized heat accumulation. This leads to the formation of microscopic hot spots and premature degradation.

The combined effects of pore oversaturation, catalytic surface activity, and enhanced local heat transfer account for the reduced thermal stability of PCM PC 15%. These results indicate that a BWC content of 10 wt.% provides the highest thermal stability. Further increases in BWC content adversely affect the resistance to thermal degradation.

Fig. 9 presents the DTG curves of PCM PP, PCM PC 5%, PCM PC 10%, and PCM PC 15% over the temperature range of 300–450 K. All samples exhibit a primary endothermic peak between 333 and 343 K, corresponding to the melting temperature of paraffin.

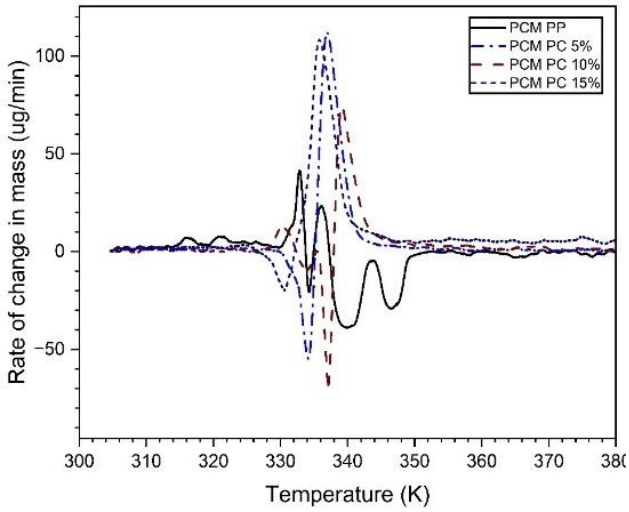

Fig. 9 DTG spectra of PCM and its composites

There are quantitative differences in peak amplitude and full width at half maximum (FWHM). These variations indicate different mass-change rates during the phase transition and reflect the thermal homogeneity of the samples.PCM-PP shows a relatively broad peak with several minor shoulders at lower temperatures, suggesting a gradual melting process and the presence of crystalline heterogeneity. Incorporation of BWC leads to a sharper peak, with PCM PC 10% displaying the sharpest peak. This signal corresponds to a localized maximum mass-change rate at the melting temperature. It reflects faster heat distribution and a more uniform phase transition. Consequently, energy transfer during paraffin melting and molecular rearrangement occurs more efficiently. In contrast, PCM PC 15% exhibits a broader peak with a reduced relative intensity. This behavior is likely caused by carbon particle agglomeration, which increases interfacial thermal resistance and reduces thermal homogeneity. As a result, the phase transition becomes more diffuse and proceeds more slowly.

These DTG results are consistent with the TGA data shown in Fig. 8, where PCM PC 10% exhibits the highest residual mass and a delayed onset of thermal decomposition. Together, these findings confirm that optimal BWC loading enhances both heat transfer efficiency and thermal durability. Similar trends have been reported for paraffin-based composites containing graphene and expandable graphite, where moderate filler contents provide the most significant thermal improvements [11].

3.5 Performance of the PCM composites

Incorporation of BWC into paraffin-based PCM significantly influences the temperature profile during electric-vehicle battery simulations. Among all compositions, PCM PC 10% maintains the lowest temperature throughout the 60-min testing period (Fig. 10(a)). Compared with natural air cooling (PA), which produces the highest temperatures, all PCM-based

strategies exhibit superior thermal regulation. A direct comparison of the temperature reduction achieved under each cooling condition relative to natural cooling is presented in Fig. 10(b).

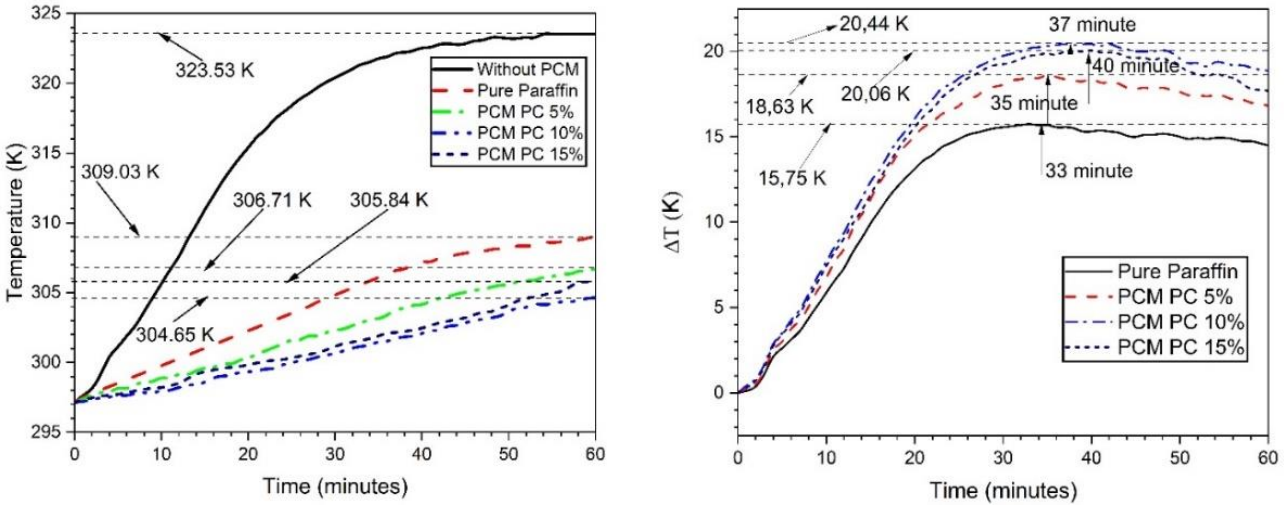

(a) Temperature profiles of the PCM composites (b) Temperature difference compared with natural cooling

Fig. 10 Cooling performance during battery simulation

The results presented in Fig. 10 do not involve an actual battery charging process; therefore, a charging-rate parameter is not applied. Instead, a constant 5-W electrical heater is used to simulate the heat generated by lithium-ion batteries during operation. This method is commonly adopted in thermal management studies because it provides a stable and controllable heat input while eliminating electrochemical effects associated with battery charging.

As shown in Fig. 10(a), PCM cooling significantly outperforms natural convection. Under natural cooling, the battery temperature reaches 323.53 K, whereas pure paraffin PCM reduces it to 309.03 K. The addition of BWC further enhances cooling performance, with PCM PC 10% achieving the lowest temperature of 304.65 K. Consistent with these results, Fig. 10(b) shows that PCM PC 10% produces the largest temperature reduction, with a peak reduction of 20.44 K at 37 min. In comparison, PCM PP provides the smallest reduction (15.75 K).

These findings agree with previous studies demonstrating that carbon-based additives can significantly improve the thermal performance of PCMs. The improvement arises from the presence of bamboo carbon within the paraffin matrix. Specifically, it increases thermal conductivity, which promotes more efficient heat absorption and distribution throughout the material [22].

Taken together, PCM PC 10% provides the most favorable balance between enhanced heat transfer and latent heat storage capacity, allowing it to maintain a lower and more stable operating temperature. In contrast, the cooling performance of PCM PC 15% declines, likely due to the reduced paraffin content, which limits latent heat storage despite faster heat transfer.

3.6 Thermal energy absorption capability

The heat energy absorption capacity of each PCM composite is quantitatively evaluated using a system-based approach through Eq. (1). This approach represents the actual heat absorption capacity of the PCM composite within a BTMS configuration. The calculations are based on a PCM mass of 300 g, consistent with the experimental setup, and the Cp of each PCM composite presented in Fig. 7. The maximum temperature difference obtained from the battery simulation between natural cooling (without PCM) and PCM-based cooling is shown in Fig. 10(b). The calculated heat absorption capacities of each PCM are presented in Fig. 11(a). Meanwhile, the heat absorption trends observed over a 60-minute operating period are illustrated in Fig. 11(b)

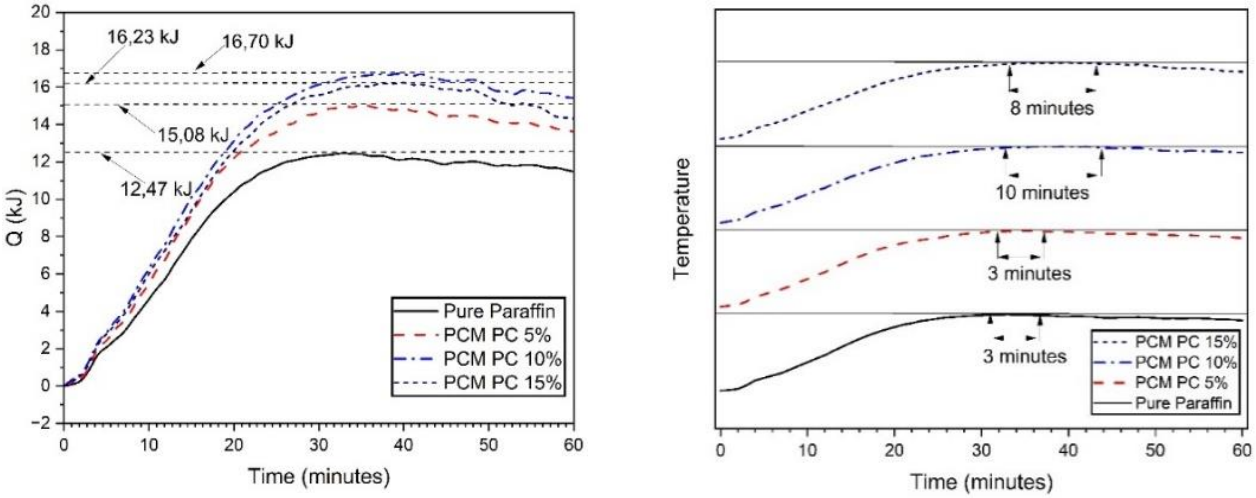

(a) Absorbed thermal energy (b) Energy absorption trends during operation

Fig. 11 Thermal energy absorption capacity of the PCM composites

Fig. 11(a) shows the amount of heat energy absorbed by each PCM composite during the battery simulation. PCM PC 10% exhibits the highest heat absorption capacity (16.70 kJ), followed by PCM PC 15% (16.23 kJ), PCM PC 5% (15.08 kJ), and PCM PP (12.47 kJ). These results confirm that the incorporation of BWC significantly enhances the ability of a paraffin-based PCM to store heat. The absorption profiles in Fig. 11(a) display a rapid increase during the first 20–30 min of operation, which is associated with the melting process of the PCM and the dominance of latent heat storage mechanisms. After this period, the curves tend to plateau, indicating that the PCM composites have approached their maximum energy storage capacity. Furthermore, Fig. 11(b) illustrates the heat absorption trends during system operation. PCM PC 10% shows the longest duration to reach its maximum heat absorption state, approximately 10 min, compared with the other PCM samples.

These findings indicate that the addition of 10 wt.% BWC provides the optimal balance between enhanced heat transfer performance and latent heat storage capacity. In contrast, at a BWC mass fraction of 15 wt.%, the total heat absorption capacity tends to decrease. This behavior is attributed to the reduction in the active paraffin fraction serving as the latent heat storage medium. There is also potential for agglomeration of carbon particles, which may reduce the effectiveness of thermal conduction pathways and hinder overall heat transfer. Collectively, these results suggest that the heat absorption capability of PCM in BTMS applications is not governed solely by latent heat values. Rather, it arises from the synergistic interaction between the Cp, thermal conductivity, and the mass of PCM involved in the cooling system.

3.7 Discussion

Modifying the characteristics of PCMs using natural materials, such as BWC, offers a promising strategy for thermal management in electric vehicle batteries. Bamboo carbon is useful as a modification material due to its intrinsic porous structure formed during carbonization, as reported in previous studies. Silvana et al. [23] reported that bamboo carbon exhibits a porous structure with a relatively large surface area and favorable thermal adsorption capability.

These findings are consistent with the experimental results of the present study. PCM PC 10% demonstrates the highest heat absorption, reflected in its maximum ΔH of all composites (Fig. 6(c)). In contrast, when the BWC mass fraction is higher or lower than 10 wt.%, the onset melting temperature and ΔH of the PCM composite are reduced. This behavior is attributed to the percolation threshold, where non-optimal filler distribution limits effective heat transfer and thermal energy storage.

Several factors govern the enhanced thermal adsorption performance of the PCM composites. First, a higher Cp within the operating temperature range enables greater sensible energy storage before and during the melting process. Second, a uniform filler distribution enhances heat transfer from the heating source, allowing for greater energy absorption. Third, pure

paraffin may contain crystalline domains that do not fully melt under dynamic heating rates. As a result, ΔH values obtained from DSC measurements do not fully translate into effective heat absorption during system-level simulations. A uniform filler distribution enhances heat transfer from the heating source, allowing for greater energy absorption. PCM PC 10% exhibits the highest ΔH and Cp, suggesting the largest heat storage capacity and the most effective heat absorption and retention capability. This behavior is consistent with the most significant battery temperature reduction observed during the simulation (Fig. 10(a)).

The agreement between laboratory characterization and system-level performance validates that 10 wt.% BWC enhances both heat storage capacity and practical cooling effectiveness. This performance improvement is attributed to the microporous structure of BWC, as observed with SEM (Fig. 5), which increases the interfacial surface area between the carbon and paraffin. The larger interfacial area improves thermal contact and facilitates more efficient local heat transfer. This synergy supports enhanced heat absorption and more effective thermal energy storage during both heating and melting processes. In addition, the carbonization process converts cellulose and lignin into activated carbon, contributing to improved structural stability and thermal efficiency [24].

The results in Fig. 11(b) indicate that PCM PC 10% can sustain maximum energy absorption for up to 10 min, which is significantly longer than PCM PP and PCM PC 5% (3 min) and PCM PC 15% (8 min). This longer absorption duration highlights the suitability of PCM PC 10% for battery thermal management. It enables rapid heat absorption while maintaining heat retention over a more extended period.Further analysis of the battery simulation results (Fig. 11), in conjunction with DSC data (Figs. 6 and 7), provides clear evidence of the thermal energy absorption behavior of the PCM composites. PCM PC 10% has the highest ΔH and Cp among all samples. These intrinsic thermal properties are directly reflected in the battery simulations, where PCM PC 10% demonstrates superior heat absorption and retention performance.

To compare the thermal energy absorption behavior among different samples, both sensible energy contributions (Cp) and effective latent energy (the mobilized portion of ΔH during simulation) are considered. Based on DSC results, the PCM composites have the following order based on the ΔH values: PCM PC 10% (104.99 kJ/kg) > PCM PP (92.45 kJ/kg) > PCM PC 15% (89.91 kJ/kg) > PCM PC 5% (84.42 kJ/kg). However, this ranking does not directly determine cooling performance under dynamic conditions. This is due to the significant influence of sensible energy storage and heating kinetics.

PCM PC 10% exhibits superior performance due to the combined effect of the highest ΔH and Cp values, resulting in the largest available thermal energy (Eavailable) within the operating temperature range of 323–348 K. This explains the most significant battery temperature reduction observed during the simulation. Though PCM PP has a relatively high ΔH, its lower Cp and potentially slower kinetic response to dynamic heating lead to less effective energy absorption over the 60-min period. Meanwhile, PCM PC 5% and PCM PC 15%, despite having lower ΔH values than PCM PP, exhibit higher Cp values and favorable initial heating kinetics. This enables greater initial sensible early uptake and, during specific time intervals, superior apparent cooling relative to PCM PP.

Although porous bamboo carbon is employed as a supporting matrix, this study does not include dedicated leakage tests to evaluate the shape stability of the paraffin-based PCM composites. The primary focus is thermal characterization using DSC and TGA, as well as system-level cooling performance evaluation for battery applications. Nevertheless, there are no signs of paraffin leakage or seepage during DSC, TGA, or battery simulation tests. Furthermore, the TGA results indicate negligible mass loss below 523 K, suggesting good thermal stability within the operating temperature range.

Based on the porous structure of BWC observed with SEM, it is expected to retain molten paraffin via capillary forces, consistent with literature reports on biocarbon-based PCMs. However, specific leakage evaluations, such as repeated heating–cooling cycles or filter paper tests, are not conducted and are acknowledged as a limitation of this study. Future work could include quantitative leakage assessments to validate the shape stability of the PCM composites.

4. Conclusions

This study successfully developed paraffin-based PCM composites enhanced with BWC, offering an effective and sustainable solution for thermal management in electric vehicle batteries. The key conclusions, implications, and significance of the findings can be summarized as follows:

(1) The incorporation of BWC at 10 wt.% into pure paraffin as a PCM composite creates a superior balance between the latent heat storage capacity and the heat transfer rate. This significantly enhances the thermal performance of the composite compared with pure paraffin.
(2) Functionally, the optimized paraffin–BWC composite overcomes a critical thermal constraint by maintaining a simulated battery temperature below 313 K for 60 min. This has important practical implications for ensuring a safer, more stable, and longer-lasting electric vehicle battery operation in line with industry standards.
(3) BWC is confirmed as a highly promising, cost-effective, and environmentally friendly thermal additive. These results highlight its potential for resource recovery and the future development of green energy storage solutions.

This research presents a robust and viable solution for next-generation BTMS. However, future studies need to focus on validating long-term cycle stability and testing performance under actual battery operating conditions to accelerate the commercialization of this material.

Acknowledgments

The authors express their gratitude to Universitas Udayana and the Material Engineering Laboratory for providing the facilities and laboratory services required throughout this research.

Conflicts of Interest

The authors declare no conflict of interest.

References

[1] Z. L. Yang, R. Walvekar, W. P. Wong, R. K. Sharma, S. Dharaskar, and M. Khalid, “Advances in Phase Change Materials, Heat Transfer Enhancement Techniques, and Their Applications in Thermal Energy Storage: A Comprehensive Review,” Journal of Energy Storage, vol. 87, article no. 111329, 2024.
[2] F. L. Rashid, M. A. Al-Obaidi, A. Dulaimi, L. F. A. Bernardo, Z. A. A. Redha, H. A. Hoshi, et al., “Recent Advances on The Applications of Phase Change Materials in Cold Thermal Energy Storage: A Critical Review,” Journal of Composites Science, vol. 7, no. 8, article no. 338, 2023.
[3] A. Takudzwa Muzhanje, M. A. Hassan, and H. Hassan, “Phase Change Material Based Thermal Energy Storage Applications for Air Conditioning: Review,” Applied Thermal Engineering, vol. 214, article no. 118832, 2022.
[4] L. Liu, J. Niu, and J. Y. Wu, “Preparation of Stable Phase Change Material Emulsions for Thermal Energy Storage and Thermal Management Applications: A Review,” Materials, vol. 15, no. 1, article no. 121, 2022.
[5] G. Z. Yin, J. Hobson, Y. Duan, and D.Y. Wang, “Polyrotaxane: New Generation of Sustainable, Ultra-Flexible, Form-Stable and Smart Phase Change Materials,” Energy Storage Materials, vol. 40, pp. 347-357, 2021.
[6] L. P. Myat, M. S. Ahmad, I. N. Pulidindi, H. Algarni, L. Kumar, A. Kalam, et al., “Effect of Polyethylene Glycol and Activated Carbon Macroparticles on Thermal Conductivity of Paraffin Wax for Thermal Storage Applications,” Polymers, vol. 14, no. 19, article no. 4181, 2022.
[7] M. Sun, T. Liu, H. Sha, M. Lin, T. Liu, X. Wang, et al., “A Review on Thermal Energy Storage with Eutectic Phase Change Materials: Fundamentals and Applications,” Journal of Energy Storage, vol. 68, article no. 107713, 2023.
[8] V. S. N. Reddy, B. N. Sai, A. S. Babu, A. Avinash, T. A. Rajesh, A. V. S. Manohar, et al., “Smart Integration of Expandable Graphite in Composite Phase Change Materials for Optimized Electric Vehicle Battery Thermal Management,” Heat Transfer, vol. 54, pp. 4745-4760, 2025.
[9] N. S. Mane, P. Kodancha, V. Hemadri, and S. Tripathi, “Investigation on Cooling Performance of Composite PCM and Graphite Fin for Battery Thermal Management System of Electric Vehicles,” Energy Storage, vol. 6, no. 6, pp. 1-16, 2024.

[10] X. Zhang, J. Huo, X. Yuan, M. Zheng, and S. Guo, "Sulfur-Free Expanded Graphite/Paraffin Composite Phase Change Material with High Thermal Conductivity for Lithium-Ion Battery Thermal Management," Journal of Thermal Science, vol. 34, no. 4, pp. 1287-1300, 2025.

[11] J. Zhao, Y. Chen, Y. Gong, and M. Chen, "A Novel Paraffin Wax/Expanded Graphite/Bacterial Cellulose Powder Phase Change Materials for the Dependable Battery Safety Management," Batteries, vol. 10, no. 10, article no. 363, 2024.

[12] Y. Huo, T. Yan, and W. Pan, "Efficient Solar Thermal Storage of Foamy Bamboo Charcoal-Based Composite Phase Change Materials," Solar Energy, vol. 268, article no. 112269, 2024.

[13] L. D. Tai and M. Y. Lee, "Advances in the Battery Thermal Management Systems of Electric Vehicles for Thermal Runaway Prevention and Suppression," Batteries, vol. 11, no. 6, article no. 216, 2025.

[14] R. Bharathiraja, T. Ramkumar, M. Selvakumar, N. Radhika, N. Praveenkumar, M. Mohanraj, et al., "Advancements in Paraffin Wax Phase Change Materials: A Comprehensive Review of Enhancement Techniques and Thermal Storage Applications," Thermochimica Acta, vol. 753, article no. 180129, 2025.

[15] M. A. Fikri, A. K. Pandey, M. Samykano, K. Kadirgama, M. George, R. Saidur, et al., "Thermal Conductivity, Reliability, and Stability Assessment of Phase Change Material (PCM) Doped with Functionalized Multi-Wall Carbon Nanotubes (FMWCNTs)," Journal of Energy Storage, vol. 50, article no. 104676, 2022.

[16] A. E. Balan, A. AL-Sharea, E. J. Lavasani, E. Tanasa, S. Voinea, B. Dobrica, et al., "Paraffin-Multilayer Graphene Composite for Thermal Management in Electronics," Materials, vol. 16, no. 6, article no. 2310, 2023.

[17] D. X. Zhang, C. Y. Zhu, B. H. Huang, X. Y. Duan, L. Gong, and M. H. Xu, "Thermal Behaviors and Performance of Phase Change Materials Embedded in Sparse Porous Skeleton Structure for Thermal Energy Storage," Journal of Energy Storage, vol. 62, article no. 106849, 2023.

[18] M. Katish, S. Allen, A. Squires, and V. Ferrandiz-Mas, "Experimental Study of Phase Change Material (PCM) Biochar Composite for Net-Zero Built Environment Applications," Cleaner Materials, vol. 14, article no. 100274, 2024.

[19] V. Saxena, S. K. Sahu, S. I. Kundalwal, and P. A. Tsai, "Optimizing Battery Thermal Management with Phase Change Materials: Influence of Thickness, Ambient Conditions, and Material Selection," Journal of Energy Storage, vol. 132, article no. 117657, 2025.

[20] W. Li, Y. Dong, X. Zhang, and X. Liu, "Preparation and Performance Analysis of Graphite Additive/Paraffin Composite Phase Change Materials," Processes, vol. 7, no. 7, article no. 447, 2019.

[21] C. Zhou, Y. Li, F. Wang, Z. Wang, Q. Xia, Y. Zhang, et al., "A Review of the Performance Improvement Methods of Phase Change Materials: Application for the Heat Pump Heating System," Energies, vol. 16, no. 6, article no. 2676, 2023.

[22] J. Cao, G. Xiao, X. Xu, D. Shen, and B. Jin, "Study on Carbonization of Lignin By TG-FTIR and High-Temperature Carbonization Reactor," Fuel Processing Technology, vol. 106, pp. 41-47, 2013.

[23] S. Alfei and O. G. Pandoli, "Bamboo-Based Biochar: A Still Too Little-Studied Black Gold and Its Current Applications," Journal of Xenobiotics, vol. 14, no. 1, pp. 416-451, 2024.

[24] J. K. Muiruri, A. C. Bonillo, M. Zhang, P. Wang, N. Tomczak, W. Wu, et al., "Sustainable Carbonized Biomass-Stabilized Phase Change Materials for Thermal Energy Storage," Journal of Energy Storage, vol. 103, article no. 114423, 2024.